

## Resonant cavity germanium photodetector via stacked single-crystalline nanomembranes

Minkyu Cho, Jung-Hun Seo, Munho Kim, Jaeseong Lee, Dong Liu, Weidong Zhou, Zongfu Yu, and Zhenqiang Ma

Citation: *Journal of Vacuum Science & Technology B* **34**, 040604 (2016); doi: 10.1116/1.4948531

View online: <http://dx.doi.org/10.1116/1.4948531>

View Table of Contents: <http://scitation.aip.org/content/avs/journal/jvstb/34/4?ver=pdfcov>

Published by the AVS: Science & Technology of Materials, Interfaces, and Processing

### Articles you may be interested in

Ultraviolet GaN photodetectors on Si via oxide buffer heterostructures with integrated short period oxide-based distributed Bragg reflectors and leakage suppressing metal-oxide-semiconductor contacts

*J. Appl. Phys.* **116**, 083108 (2014); 10.1063/1.4894251

Resonant cavity-enhanced quantum-dot infrared photodetectors with sub-wavelength grating mirror

*J. Appl. Phys.* **113**, 213108 (2013); 10.1063/1.4809574

High speed photodetectors based on a two-dimensional electron/hole gas heterostructure


*Appl. Phys. Lett.* **102**, 161108 (2013); 10.1063/1.4802595





1.55  $\mu\text{m}$  GaInNAs resonant-cavity-enhanced photodetector grown on GaAs

*Appl. Phys. Lett.* **87**, 111105 (2005); 10.1063/1.2048828

High-speed Si resonant cavity enhanced photodetectors and arrays

*J. Vac. Sci. Technol. A* **22**, 781 (2004); 10.1116/1.1647591


Instruments for Advanced Science

<p>Contact Hiden Analytical for further details:  <b>W</b> <a href="http://www.HidenAnalytical.com">www.HidenAnalytical.com</a>  <b>E</b> <a href="mailto:info@hiden.co.uk">info@hiden.co.uk</a>  <a href="#">CLICK TO VIEW</a> our product catalogue</p>	 <p><b>Gas Analysis</b></p> <ul style="list-style-type: none"> <li>› dynamic measurement of reaction gas streams</li> <li>› catalysis and thermal analysis</li> <li>› molecular beam studies</li> <li>› dissolved species probes</li> <li>› fermentation, environmental and ecological studies</li> </ul>	 <p><b>Surface Science</b></p> <ul style="list-style-type: none"> <li>› UHV TPD</li> <li>› SIMS</li> <li>› end point detection in ion beam etch</li> <li>› elemental imaging - surface mapping</li> </ul>	 <p><b>Plasma Diagnostics</b></p> <ul style="list-style-type: none"> <li>› plasma source characterization</li> <li>› etch and deposition process reaction</li> <li>› kinetic studies</li> <li>› analysis of neutral and radical species</li> </ul>	 <p><b>Vacuum Analysis</b></p> <ul style="list-style-type: none"> <li>› partial pressure measurement and control of process gases</li> <li>› reactive sputter process control</li> <li>› vacuum diagnostics</li> <li>› vacuum coating process monitoring</li> </ul>
---	--	--	--	--

# Resonant cavity germanium photodetector via stacked single-crystalline nanomembranes

Minkyu Cho,<sup>a)</sup> Jung-Hun Seo, Munho Kim, Jaeseong Lee, and Dong Liu  
 Department of Electrical and Computer Engineering, University of Wisconsin-Madison, Madison,  
 Wisconsin 53706

Weidong Zhou  
 Department of Electrical Engineering, University of Texas at Arlington, Arlington, Texas 76019

Zongfu Yu and Zhenqiang Ma<sup>b)</sup>  
 Department of Electrical and Computer Engineering, University of Wisconsin-Madison, Madison,  
 Wisconsin 53706

(Received 9 March 2016; accepted 20 April 2016; published 2 May 2016)

In this paper, the authors report resonant cavity (RC) metal-semiconductor-metal (MSM) germanium nanomembrane (Ge NM) photodetectors via transfer printing. The dislocation-free Ge NM layer was transferred onto an ultrathin Si NM/SiO<sub>2</sub> distributed Bragg reflector. As a result, a low dark current density of  $1 \times 10^{-9}$  A/ $\mu\text{m}^2$  and a quantum efficiency of 17.3% at 1.55  $\mu\text{m}$ , which is twice larger than the quantum efficiency without a bottom mirror, were measured from the transferred RC MSM Ge photodetector. The enhancement of the quantum efficiency is verified by simulation. © 2016 American Vacuum Society. [<http://dx.doi.org/10.1116/1.4948531>]

## I. INTRODUCTION

A high efficiency, low-cost data communication system is desirable in the near future. In that sense, the combination of full monolithic Si integrated circuits with optical devices pose great potentials as one of the most prominent candidates for a high-speed communication system. Si photonics is a widely studied field among researchers due to its low-cost and compatibility to the current CMOS process.<sup>1,2</sup> However, Si is not suitable as an absorbing material in the near-infra regime due to its transparency in 1.3–1.5  $\mu\text{m}$  wavelength. The small bandgap, 0.67 eV, of germanium (Ge) makes it suitable for 1.3–1.55  $\mu\text{m}$  optical communication systems. Therefore, it is highly desirable to integrate high quality Ge on Si-based systems. Attempts to integrate Ge onto Si have been made through wafer bonding process or, most notably, epitaxial growth.<sup>3</sup> The growth of high quality Ge on Si has been a challenge since the lattice mismatch between Si and Ge is 4%, and this causes threading dislocation within the Ge. The misfit/threading dislocations generated during the epitaxial growth process degrade performance of the electrical device, increasing leakage current. To reduce threading dislocation and other defects in Ge during the growth process, growing SiGe beforehand as a buffer layer was proposed.<sup>4</sup> This method effectively reduced the dislocation density, but growing a thick buffer layer further adds to process complexities. To grow Ge directly on Si, a two-step ultra-high vacuum/chemical-vapor-deposition process followed by cyclic annealing was proposed.<sup>5</sup> However, this method could result in intermixing between Si and Ge during the annealing process.<sup>6</sup>

Recent advances in transfer printing of a single crystalline nanomembrane (NM) provide access to form single crystalline nanomembranes on unconventional substrates.<sup>7,8</sup> Due to a single crystalline nature of the nanomembrane, this transfer printing method enabled by using an elastomeric stamp offers not only an atomically smooth surface but also a clean interface, even when NMs are stacked. Several optical/electrical devices previously demonstrated with this method showed high yields.<sup>9–13</sup>

In this work, resonant cavity (RC) metal-semiconductor-metal (MSM) Ge photodetectors by the NM transfer printing method was demonstrated. The Ge NM layer, released from a smart-cut processed germanium-on-insulator wafer,<sup>14</sup> was directly transferred onto the Si NM/SiO<sub>2</sub> distributed Bragg reflector (DBR). Therefore, a high quality Ge NM, free from misfit/threading dislocations, was obtained. High reflectivity bottom DBR mirror increases the quantum efficiency of the photodetector with a thin Ge absorbing layer. While many RC Ge photodetectors with superior performances were reported from literatures,<sup>15–17</sup> the transfer method is seamlessly applicable to the known resonant Ge photodetector designs.

## II. EXPERIMENT

The fabrication process began with a silicon-on-insulator (SOI) with 234 nm of top Si layer and 2000 nm of buried oxide (BOX) layer. The SOI was patterned with photoresist followed by SF<sub>6</sub>/O<sub>2</sub> reactive ion etching to remove the exposed Si top layer to define the Si NM shape. After etching, the sample was immersed in concentrated hydrofluoric acid to remove the BOX layer and release Si NM from the substrate. The detailed process of Si NM preparation can be found in other literatures.<sup>12,18</sup>

The released Si NM was rinsed with deionized water and transferred via a polydimethylsiloxane (PDMS) stamp onto a receiver substrate (quartz), as shown in Figs. 1(a) and 1(b).

<sup>a)</sup>Present address: Department of Mechanical Engineering, Korea Advanced Institute of Science and Technology (KAIST), 291 Daehak-ro, Yuseong-gu, Daejeon 305-701, Korea.

<sup>b)</sup>Author to whom correspondence should be addressed; electronic mail: mazq@engr.wisc.edu

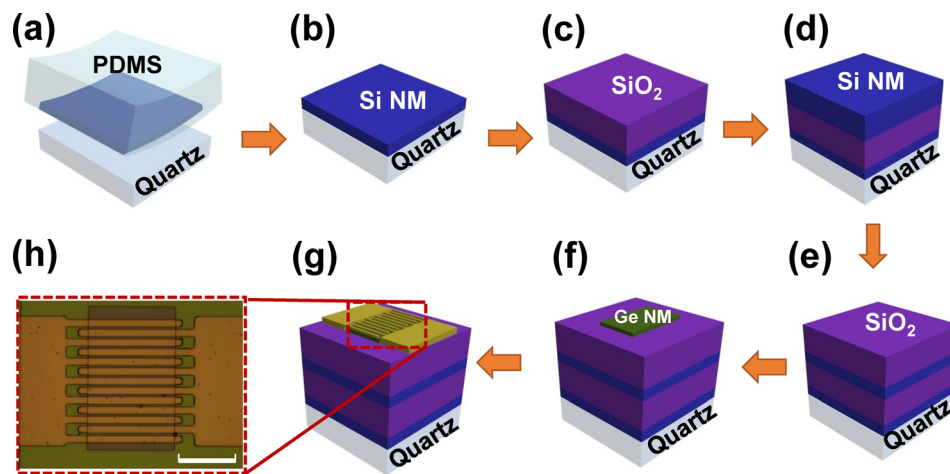


FIG. 1. (Color online) Schematic illustrations of the fabrication process for the RC MSM Ge photodetectors. (a) Transfer Si NM with PDMS stamp, (b) transferred Si NM on a quartz substrate, (c) thermal oxidation after first Si NM, (d) second Si NM transfer after one-pair Si/SiO<sub>2</sub> DBR, (e) second thermal oxidation, (f) transferred Ge NM on two-pairs Si/SiO<sub>2</sub> DBR, (g) complete device after Ti/Au electrode deposition and lift-off, and (h) optical microscope image of the RC MSM Ge photodetector. The scale bar is 50  $\mu\text{m}$ .

The transferred Si NM was partially oxidized by a wet oxidation process [Fig. 1(c)]. The thicknesses of SiO<sub>2</sub> and Si NM after oxidation were 270 and 110 nm, respectively, which were confirmed by both reflectivity measurement and SEM cross section image.<sup>11</sup> The NM transfer and oxidation processes were repeated again until a two-pair DBR structure was obtained, as shown in Figs. 1(d) and 1(e). After the second oxidation, 570 nm thick Ge NM was transferred onto the two-pair Si/SiO<sub>2</sub> DBR, as shown in Fig. 1(f). The entire sample was annealed with a rapid thermal annealing system for 5 min at 250 °C to increase the bonding strength between Ge NM and SiO<sub>2</sub>. Finally, Ti/Au (10 nm/500 nm) was deposited as anode and cathode contact metals, as shown in Fig. 1(g). As a comparison, MSM Ge photodetector on quartz substrate was also fabricated. Figure 1(h) shows the optical microscope image of the completed device. The width and spacing between metal electrodes are 5 and 2  $\mu\text{m}$ , respectively.

### III. RESULTS AND DISCUSSION

The quantum efficiency of the RC photodetector is estimated by the following equation:<sup>18</sup>

$$\eta = \left\{ \frac{(1 + R_2 e^{-\alpha L})}{1 - 2\sqrt{R_1 R_2} e^{-\alpha L} \cos(2\beta L + \psi_1 + \psi_2) + R_1 R_2 e^{-2\alpha L}} \right\} \times (1 - R_1)(1 - e^{-\alpha L}), \quad (1)$$

where  $R_1$  and  $R_2$  are top and bottom reflectivities,  $\alpha$  is the absorption coefficient,  $L$  is the thickness of the active layer,  $\psi_1$  and  $\psi_2$  are top and bottom mirror phase shifts, and  $\beta$  is the propagation constant. Based on Eq. (1), the quantum efficiency ( $\eta$ ) of the RC photodetector by different Ge layer thicknesses and wavelengths are simulated, as shown in Figs. 2(a) and 2(b). As a result, the quantum efficiency of the RC Ge photodetector is periodically increased as the Ge thickness is increased. With a Ge thickness of 570 nm, the theoretical maximum quantum efficiency is located at 1.52  $\mu\text{m}$  and decreased as the wavelength deviated from the 1.52  $\mu\text{m}$  region. Based on the simulations, 79% of quantum efficiency is expected at 1.55  $\mu\text{m}$  for the Ge photodetector on Si/SiO<sub>2</sub> DBR and 40% for the Ge photodetector on a quartz substrate. The quantum efficiency of the RC Ge photodetector with DBR is about two times larger than the quantum efficiency for the one on quartz substrate. This simulation was based on the assumption that all the photogenerated carriers

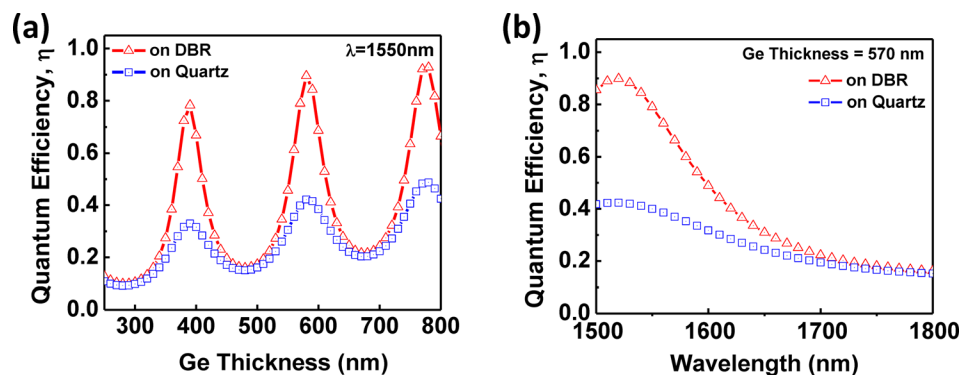


FIG. 2. (Color online) Simulated quantum efficiency of the RC MSM Ge photodetector and a Ge photodetector on a quartz substrate. (a) Quantum efficiency vs Ge thickness. (b) Quantum efficiency vs wavelength.

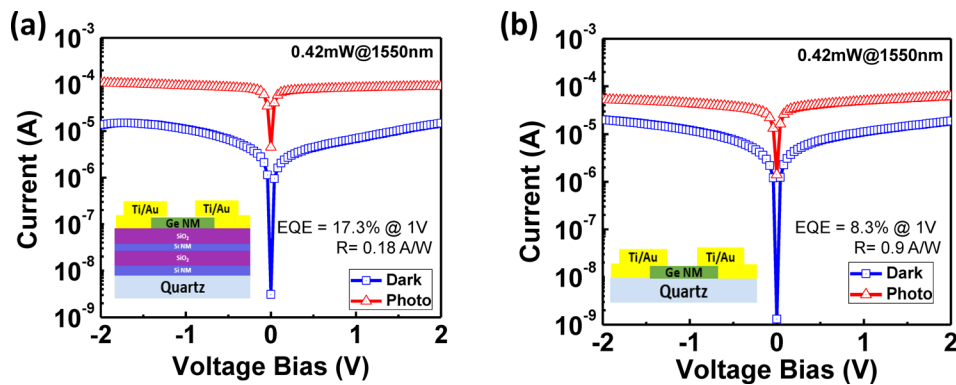


FIG. 3. (Color online) Measured photo/dark current of (a) the RC MSM Ge photodetector and (b) the MSM Ge photodetector on quartz substrate.

contribute to the detector current.<sup>19</sup> It should be noted that the electrodes' periodicity is  $7\ \mu\text{m}$ , suggesting that the electrodes induced polarization is negligible for the target wavelength ( $1.55\ \mu\text{m}$ ).

To verify the simulation results, the dark and photocurrent of the Ge photodetectors were measured, as shown in Figs. 3(a) and 3(b). A tunable laser source is connected to a lensed fiber to couple the light into the photodetectors for the photocurrent measurement. As a result, responsivities of 0.18 and 0.09 A/W were measured at  $1.55\ \mu\text{m}$  under 1 V for the MSM photodetector on DBR and the one on quartz, respectively. Even without adopting special Schottky barrier enhancement layers, transferred MSM Ge photodetectors show very low level of dark current of  $1 \times 10^{-9}\ \text{A}/\mu\text{m}^2$  at 1 V compared to Ge MSM photodetectors from other literature.<sup>20–22</sup>

Figures 4(a) and 4(b) show the photocurrent versus light intensity for different voltage biases. As expected, the photocurrent increased proportionally with the light intensity and the voltage bias. The measured quantum efficiencies of 17.3% and 8.3% were measured for the MSM Ge photodetector on DBR and that on quartz, respectively. It is found that the employment of DBR as a bottom mirror enhanced the quantum efficiency by twofold. This result matches well with the theoretical prediction. The lower measured quantum efficiency compared to the theoretical one could be attributed to the possibility that the photogenerated carriers were not collected to the electrodes due to recombination sites in

the Ge layer. Another possibility is the shadow effect due to the thick electrodes (520 nm) by which a fair amount of light could not enter the devices. Using thinner metal or transparent metal electrodes could increase the quantum efficiency of the device.

Although the measured quantum efficiency values are less than the theoretical ones, the quantum efficiency of the NM-transferred RC Ge photodetector is comparable to other conventional RC Ge photodetectors with a given Ge thickness at  $1.55\ \mu\text{m}$ .<sup>3,21</sup> The theoretical and measured quantum efficiencies at different wavelengths are compared, as shown in Fig. 5. The calculated and measured quantum efficiencies show large differences due to the low coupling efficiency by the shadow effect of the metal electrodes as mentioned earlier. However, both calculated and measured results show the decreasing trend of the quantum efficiencies from  $1.52$  to  $1.56\ \mu\text{m}$ .

#### IV. SUMMARY AND CONCLUSION

In summary, an RC MSM Ge photodetector was demonstrated by using the NM transfer printing method. The MSM Ge photodetectors were fabricated both on DBR and quartz substrates, and the simulated and measured quantum efficiencies were compared. As a result, a low dark current density of  $1 \times 10^{-9}\ \text{A}/\mu\text{m}^2$  and a quantum efficiency of 17.3% (responsivity = 0.18 A/W) were obtained at  $1.55\ \mu\text{m}$  from the RC Ge photodetector, which is about two times greater

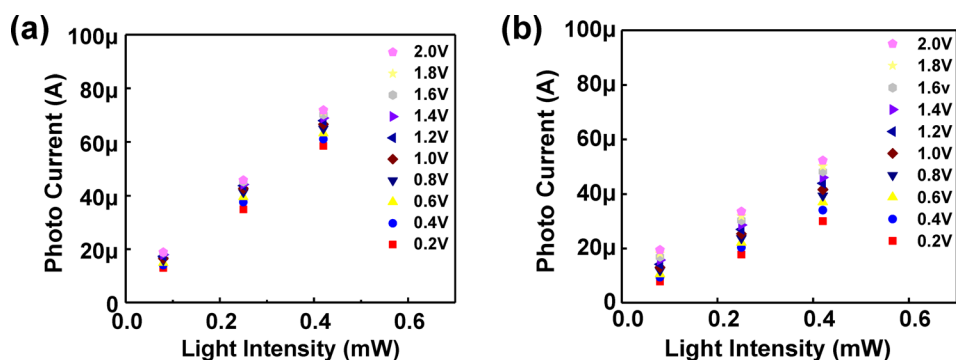


FIG. 4. (Color online) Photocurrent vs light intensity at  $1.55\ \mu\text{m}$  with different voltage biases of (a) the RC MSM Ge photodetector and (b) the Ge MSM Ge photodetector on a quartz substrate.

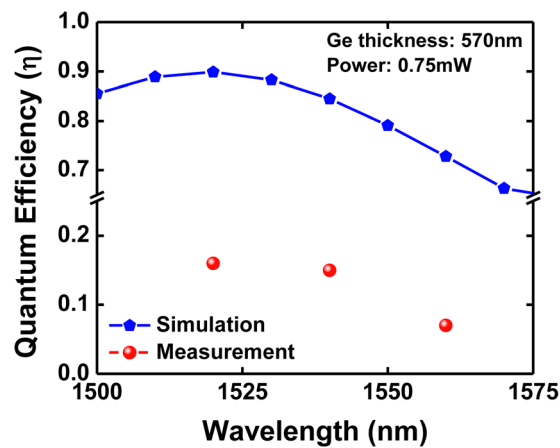


FIG. 5. (Color online) Comparison of the simulated and measured quantum efficiencies of the RC MSM Ge photodetector for different wavelengths.

than that for the MSM photodetector on quartz substrate (quantum efficiency = 8.3%, responsivity = 0.09 A/W).

## ACKNOWLEDGMENT

This work was supported by AFOSR under a PECASE Grant No. FA9550-09-1-0482. The program manager is Gernot Pomrenke.

<sup>1</sup>B. Jalali and S. Fathpour, *J. Lightwave Technol.* **24**, 4600 (2006).

<sup>2</sup>R. Soref, *Nat. Photonics* **4**, 495 (2010).

- <sup>3</sup>O. I. Dosunmu, D. D. Cannon, M. K. Emsley, B. Ghyselen, L. Jifeng, L. C. Kimerling, and M. S. Ünlü, *IEEE J. Sel. Top. Quantum Electron.* **10**, 694 (2004).
- <sup>4</sup>O. Jungwoo, J. C. Campbell, S. G. Thomas, S. Bharatan, R. Thoma, C. Jasper, R. E. Jones, and T. E. Zirkle, *IEEE J. Quantum Electron.* **38**, 1238 (2002).
- <sup>5</sup>H.-C. Luan, D. R. Lim, K. K. Lee, K. M. Chen, J. G. Sandland, K. Wada, and L. C. Kimerling, *Appl. Phys. Lett.* **75**, 2909 (1999).
- <sup>6</sup>K. H. Lee, S. Bao, G. Y. Chong, Y. H. Tan, E. A. Fitzgerald, and C. S. Tan, *APL Mater.* **3**, 016102 (2015).
- <sup>7</sup>M. A. Meitl, Z.-T. Zhu, V. Kumar, K. J. Lee, X. Feng, Y. Y. Huang, I. Adesida, R. G. Nuzzo, and J. A. Rogers, *Nat. Mater.* **5**, 33 (2006).
- <sup>8</sup>A. Carlson, S. Wang, P. Elvikis, P. M. Ferreira, Y. Huang, and J. A. Rogers, *Adv. Funct. Mater.* **22**, 4476 (2012).
- <sup>9</sup>H. Yang *et al.*, *Nat. Photonics* **6**, 615 (2012).
- <sup>10</sup>J.-H. Seo, K. Zhang, M. Kim, D. Zhao, W. Zhou, and Z. Ma, *Adv. Opt. Mater.* **4**, 120 (2016).
- <sup>11</sup>M. Cho, J.-H. Seo, J. Lee, D. Zhao, H. Mi, X. Yin, X. Wang, W. Zhou, and Z. Ma, *Appl. Phys. Lett.* **106**, 181107 (2015).
- <sup>12</sup>W. Zhou *et al.*, *Prog. Quantum Electron.* **38**, 1 (2014).
- <sup>13</sup>M. Cho *et al.*, *J. Vac. Sci. Technol., B* **34**, 040601 (2016).
- <sup>14</sup>B. Michel, A. Bernard, and A.-H. Andre-Jacques, *Jpn. J. Appl. Phys., Part 1* **36**, 1636 (1997).
- <sup>15</sup>D. Feng *et al.*, *Appl. Phys. Lett.* **95**, 261105 (2009).
- <sup>16</sup>L. Chen and M. Lipson, *Opt. Express* **17**, 7901 (2009).
- <sup>17</sup>K. C. Balram, R. M. Audet, and D. A. B. Miller, *Opt. Express* **21**, 10228 (2013).
- <sup>18</sup>K. Zhang, J.-H. Seo, W. Zhou, and Z. Ma, *J. Phys. D: Appl. Phys.* **45**, 143001 (2012).
- <sup>19</sup>M. S. Ünlü and S. Strite, *J. Appl. Phys.* **78**, 607 (1995).
- <sup>20</sup>K. W. Ang, S. Y. Zhu, J. Wang, K. T. Chua, M. B. Yu, G. Q. Lo, and D. L. Kwong, *IEEE Electron Device Lett.* **29**, 704 (2008).
- <sup>21</sup>J. Oh, S. K. Banerjee, and J. C. Campbell, *IEEE Photonics Technol. Lett.* **16**, 581 (2004).
- <sup>22</sup>A. K. Okyay, A. M. Nayfeh, K. C. Saraswat, T. Yonehara, A. Marshall, and P. C. McIntyre, *Opt. Lett.* **31**, 2565 (2006).